

# CARL: Congestion-Aware Reinforcement Learning for Imitation-based Perturbations in Mixed Traffic Control

Bibek Poudel<sup>1</sup>, Weizi Li<sup>1</sup>, and Shuai Li<sup>2</sup>

**Abstract**—Human-driven vehicles (HVs) exhibit complex and diverse behaviors. Accurately modeling such behavior is crucial for validating Robot Vehicles (RVs) in simulation and realizing the potential of mixed traffic control. However, existing approaches like parameterized models and data-driven techniques struggle to capture the full complexity and diversity. To address this, in this work, we introduce CARL, a hybrid approach that combines imitation learning for close proximity car-following and probabilistic sampling for larger headways. We also propose two classes of RL-based RVs: a safety RV focused on maximizing safety and an efficiency RV focused on maximizing efficiency. Our experiments show that the safety RV increases Time-to-Collision above the critical 4 second threshold and reduces Deceleration Rate to Avoid a Crash by up to 80%, while the efficiency RV achieves improvements in throughput of up to 49%. These results demonstrate the effectiveness of CARL in enhancing both safety and efficiency in mixed traffic.

## I. INTRODUCTION

Robot Vehicles (RVs) have the potential to revolutionize transportation by enhancing safety, efficiency, and accessibility for all road users [1]. To fully realize the benefits of this technology, it is crucial to validate their robustness through comprehensive testing [2]. While real-world evaluation is essential, it involves significant risks, costs, and time constraints, making simulation a safer, more efficient, and cost-effective alternative [3]. Nevertheless, the validation of RVs in simulation faces the challenge of accurately modeling the behaviors of Human-driven Vehicles (HVs) [4]. As more vehicles with varying levels of autonomy are introduced into our transportation system, the idea of *mixed traffic control*, which involves the use of RVs to mitigate problems such as congestion and delays produced by HVs, has emerged [5]–[11]. In mixed traffic scenarios where RVs and HVs co-exist, accurately modeling real-world human driving behavior becomes even more critical. However, this remains an open problem [12].

Among the various aspects of real-world human driving, longitudinal car-following is the most prevalent [13]. Consequently, accurate modeling of car-following behavior is crucial for reproducing realistic traffic flows and vehicle interactions in simulation, and is a key component in addressing the *sim-2-real* gap [14]. To reproduce the car-following behaviors of HVs in simulation, there exist two mainstream methods: parameterized models and data-driven

<sup>1</sup>Bibek Poudel and Weizi Li are with Min H. Kao Department of Electrical Engineering and Computer Science at University of Tennessee, Knoxville, TN, USA [bpoudel13@vols.utk.edu](mailto:bpoudel13@vols.utk.edu), [weizili@utk.edu](mailto:weizili@utk.edu)

<sup>2</sup>Shuai Li is with Department of Civil and Environmental Engineering at University of Tennessee, Knoxville, TN, USA [sli48@utk.edu](mailto:sli48@utk.edu)

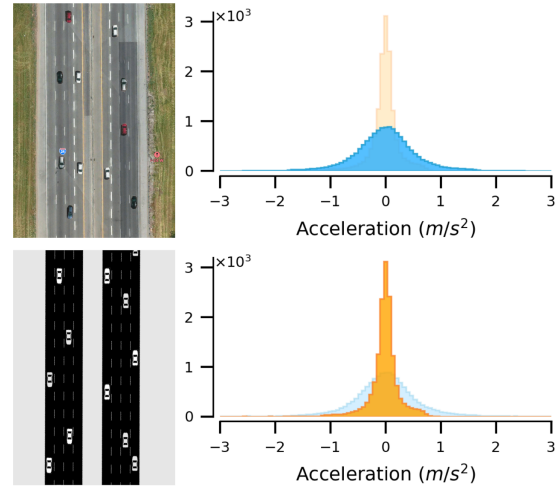


Fig. 1: Instantaneous accelerations observed during car-following behaviors at densities  $[70, 150]$  *veh/km*. TOP: Real-world data from the I-24 MOTION dataset reveals a distribution having long tails extending to  $[-3, 3]$   $m/s^2$ . BOTTOM: IDM (in simulation) produces accelerations mostly within  $[-0.5, 0.5]$   $m/s^2$ , indicating much ‘timid’ driving behaviors than the real world.

approaches. Popular parameterized car-following models, such as Gipp’s [15], Krauss’ [16], and the Intelligent Driver Model (IDM) [17], rely on calibrating various parameters (typically include maximum acceleration, minimum time gap, and desired velocity) to accurately represent driving behaviors and vehicle dynamics. However, the performance of these models heavily depends on the quality of calibration, and even with robust calibration, they may still fall short in capturing traffic diversity and lack broad applicability [18]. Enhancements to the IDM model (often a default choice in simulations like SUMO [19]) by addition of random noise [20] and tuning with real-world data [21], [22] have been proposed, but they struggle to reproduce real-world variability [23] and fail to generalize outside the reference datasets [24]. Fig. 1 illustrates a typical example, where the IDM with random noise model fails to capture the long-tailed distribution of accelerations observed in real-world data, exhibiting a 24% discrepancy (between real-world and simulation) in the percentage of accelerations observed within  $[-0.5, 0.5]$   $m/s^2$ , i.e., depicting primarily safe or timid behaviors in simulation. Further, prior studies in traffic control and coordination often impose artificial limits on vehicle behaviors, such as bounded accelerations [25]–[29], which further reduce the accuracy of simulated HVs.

Data-driven approaches such as supervised learning and Reinforcement Learning (RL) have surpassed IDM in car-

following simulation accuracy [30]. These techniques train neural networks on features extracted from real-world data [30] or use the data to tune the reward function in RL [31], [32]. Some RL-based approaches also equip HVs with both leader and follower vehicle information [33]. However, these methods still face challenges in capturing the full complexity of human driving, as they often require hand-crafted features and extensive training and tuning [34]. Imitation Learning (IL) offers a promising alternative to address these shortcomings. By learning directly from expert demonstrations, IL captures the implicit knowledge and individual preferences of human drivers, such as safety and comfort, without the need to specify these objectives. In addition, IL models can be more robust under environmental uncertainties and disturbances, as the expert’s behavior may already account for these factors [35]. While IL shows great potential, relying solely on it may still not be sufficient to capture the full spectrum of human driving behaviors and reactions as IL may overfit and struggle to generalize outside the training distribution [36].

To address these limitations, we introduce CARL, a hybrid technique that combines imitation learning and probabilistic sampling. The key difference in our work is that we consider the proximity between HVs during car-following to be a crucial factor in determining the appropriate acceleration model. When HVs are at close proximity to a leader HV during car-following, their accelerations are obtained from the imitation learning model, which captures the nuances of human driving behavior in these more sensitive situations, as the consequences of small changes in accelerations are more profound and potentially dangerous. Conversely, when the space headway exceeds a threshold, we employ probabilistic sampling to generate accelerations that introduce realistic variability. This hybrid approach enables CARL to produce more accurate representations of real-world driving behaviors, including aggressive acceleration profiles. CARL leverages the strengths of both machine learning methods, which offer accurate representations of real-world driving behaviors, and probabilistic sampling, which minimizes approximations and assumptions. In addition, we propose two classes of RL-based RVs: a *safety* RV focused on maximizing safety and an *efficiency* RV focused on maximizing efficiency. Our RVs are designed to optimize their actions based on the congestion conditions predicted by a supervised classifier, whose output is incorporated into the observation and reward of the RL algorithm.

Under the realistic-accelerations we evaluate the safety and efficiency and compare CARL with RVs proposed in prior studies for mixed traffic control. To evaluate safety, we use two surrogate measures, time to collision (TTC  $\uparrow$ ) and deceleration rate to avoid a crash (DRAC  $\downarrow$ ) whereas for efficiency we measure fuel economy (FE  $\uparrow$ ) and throughput ( $\uparrow$ ). Our experiments show that our RV consistently outperforms other methods in safety, increasing TTC above 4 s and reducing DRAC by up to 80%. Whereas in efficiency our RV achieves improvements of up to 49% in throughput while also consistently maintaining the second-

highest fuel economy among all evaluated methods. These results show that CARL effectively improves both safety and efficiency in mixed traffic. To the best of our knowledge, CARL is the first work to address the crucial gap between simulated and real-world car-following behaviors using a hybrid imitation learning approach, and to leverage congestion-aware RL for optimizing mixed traffic control. The project code can be found in the repository: <https://github.com/poudel-bibek/CARL>.

## II. METHODOLOGY

We introduce our data processing procedure, Intelligent Driver Model (IDM), Model-based and Heuristic-based RVs, our RL-based RV, and the imitation of real-world driving behaviors and perturbations.

### A. Data Processing and Intelligent Driver Model (IDM)

We apply a car-following-filter [24] to the I-24 MOTION dataset [37] with 6.75 km study length and 4 h study time. The dataset contains different vehicle types such as semi-trailers, mid-sized trucks, motorbikes, and cars under various traffic conditions such as approaching standing traffic, lane changing, and free flow. To extract car-following trajectories, we select data points that meet the following criteria:

- Ego car is following another car, i.e., has a leader.
- Leader and ego cars are in the same lane  $\geq 5$  s.
- Ego car’s speed is  $> 10\%$  of the speed limit, i.e., not approaching stationary traffic.
- Ego car’s space headway is  $< 124$  m, applying 4 s rule at the speed limit to avoid free flow conditions.

By applying the filter, we extract a total of 172,000 instantaneous accelerations, their distribution is shown in Fig.1 TOP. In comparison, Fig. 1 BOTTOM depicts the accelerations obtained from the IDM car-following model, which assumes that drivers strive to maintain a safe distance from the leader vehicle while trying to achieve a target speed. In IDM, vehicles speed up when the distance to the leading vehicle is substantial, and decelerate when the distance decreases below a target minimum gap. The parameters of IDM are set according to Treiber and Kesting [17] as maximum acceleration ( $a$ ) = 1, maximum deceleration ( $b$ ) = 1.5, target time headway ( $T$ ) = 1, acceleration coefficient ( $\delta$ ) = 4, and minimum gap ( $s_0$ ) = 2.

### B. Heuristic-based Robot Vehicles

FollowerStopper (FS): FS [38] is an RV that travels at a fixed command velocity (target) under safe conditions but when required, slightly lowers the target velocity to open a gap to the leader vehicle. This allows the RV to dampen oscillations and brake smoothly when needed. The command velocity is given by

$$v_{cmd} = \begin{cases} 0, & \text{if } \Delta x \leq \Delta x_1 \\ v \frac{\Delta x - \Delta x_1}{\Delta x_2 - \Delta x_1}, & \text{if } \Delta x_1 < \Delta x \leq \Delta x_2 \\ v + (U - v) \frac{\Delta x - \Delta x_2}{\Delta x_3 - \Delta x_2}, & \text{if } \Delta x_2 < \Delta x \leq \Delta x_3 \\ U, & \text{if } \Delta x_3 < \Delta x \end{cases}$$

where  $v = \min(\max(v_{\text{lead}}, 0), U)$  is the speed of the leader vehicle,  $\Delta x$  is the headway of the RV, and  $U$  is the desired velocity. The thresholds  $(\Delta x_1, \Delta x_2, \Delta x_3)$  are defined as

$$\Delta x_k = \Delta x_k^0 + \frac{1}{2d_k}(\Delta v_-)^2, \quad k = 1, 2, 3.$$

The model parameters  $\Delta x_k^0$ ,  $\Delta v_-$ , and  $d_k$  together determine the spacing between vehicles and the RV's responsiveness to changes in velocity.

Proportional-integral with saturation (PIwS): PIwS [38] estimates the desired average velocity ( $U$ ) of the vehicles in the network using its historical average velocity. The PIwS RV calculates the target velocity as

$$v_{\text{target}} = U + v_{\text{catch}} \times \min\left(\max\left(\frac{\Delta x - g_l}{g_u - g_l}, 0\right), 1\right),$$

which is used to calculate the command velocity at  $t + 1$

$$v_{\text{cmd}}^{t+1} = \beta_t(\alpha_t v_{\text{target}}^t + (1 - \alpha_t)v_{\text{lead}}^t) + (1 - \beta_t)v_{\text{cmd}}^t,$$

where  $v_{\text{catch}}$  is the catch-up velocity—a velocity higher than the average velocity allows the RV to catch up with its leader,  $\Delta x$  is the difference in position between the RV and its leader,  $g_l$  and  $g_u$  represent the lower and upper threshold distance, respectively;  $\alpha_t$  and  $\beta_t$  represent the weight factors for target velocity  $v_{\text{target}}$  and command velocity  $v_{\text{cmd}}$ , respectively. Finally,  $v_{\text{lead}}$  represents leader vehicle velocity.

### C. Model-based Robot Vehicles

Bilateral Control Module (BCM): BCM [39] uses information about both follower and leader vehicles to obtain a linear model whose acceleration is given by:

$$a = k_d \cdot \Delta_d + k_v \cdot (\Delta v_l - \Delta v_f) + k_c \cdot (v_{\text{des}} - v),$$

where  $\Delta_d$ ,  $\Delta v_l$ ,  $\Delta v_f$ ,  $v_{\text{des}}$ , and  $v$ , represent the difference in distance to the leader compared to the distance to the follower, the difference in velocity to the leader, the difference in velocity to the follower, the set desired velocity, and the current velocity of the vehicle, respectively.  $k_d = 1$ ,  $k_v = 1$ , and  $k_c = 1$  are gain parameters.

Linear Adaptive Cruise Control (LACC): LACC is an improvement over existing cruise control systems that allows vehicles to maintain a safe distance or speed without communication. One implementation is the constant time-headway model by Rajamani [40], which employs a first-order differential equation for approximation. The control acceleration at time  $t$  is given by

$$a_t = \left(1 - \frac{\Delta t}{\tau}\right) \cdot a_{(t-1)} + \frac{\Delta t}{\tau} \cdot a_{\text{cmd},(t-1)},$$

$$a_{\text{cmd}} = k_1 \cdot e_x + k_2 \cdot \Delta v_l, \quad \text{and } e_x = s - h \cdot v,$$

where  $k_1 = 0.3$  and  $k_2 = 0.4$  are design parameters,  $e_x$  is the gap error,  $s$  is the space headway,  $\Delta v_l$  is the relative velocity difference to the leader,  $h = 1$  is the desired time gap,  $\Delta t$  is the control time-step, and  $\tau = 0.1$  is the time lag of the control system.

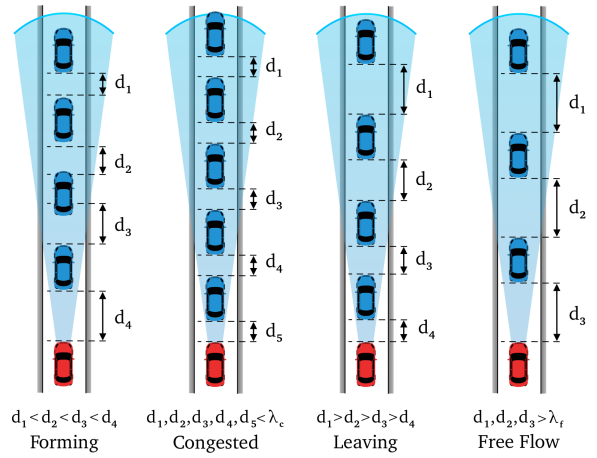


Fig. 2: Input data labeling for the congestion classifier (sensing zone shown in blue). The congestion classifier takes as input (position, velocity) of all vehicles in the sensing zone and outputs the traffic condition based on patterns in space headway.

### D. RL-based Robot Vehicles

RL is a  $T$ -step episodic task where an agent interacts with its environment to maximize the sum of discounted rewards. At each time step, the agent receives a state  $s$ , takes an action  $a$ , and the environment returns the next state  $s'$  and reward  $r$ . This is formalized as a Partially Observable Markov Decision Process represented as  $(\mathcal{S}, \mathcal{A}, \mathcal{P}, \mathcal{R}, \Omega, \mathcal{O}, \gamma)$ , where  $\mathcal{S}$  is the set of states,  $\mathcal{A}$  is the set of actions,  $\mathcal{P}(s', r|s, a)$  describes the environment dynamics,  $\mathcal{R}(s, a)$  is the reward function,  $\Omega$  is the set of observations,  $\mathcal{O}(o|s', a)$  is the observation function, and  $\gamma$  is the discount factor. RL-based methods have gained popularity as an effective alternative to model-based or heuristic-based methods.

Safety and efficiency goals often conflict in driving scenarios [31]; for example, optimizing for throughput may lead to reduced space headways and increased velocities, which can compromise safety. To address this trade-off, we propose two types of RVs: the *safety* RV, which prioritizes safety, and the *efficiency* RV, which emphasizes efficiency. Both RV types use the congestion classifier and operate within the same action and observation space. We train our RVs using the PPO algorithm [41] with the following MDP components:

- **Observation.** The RV's observation  $o_t$  at time  $t$  is a combination of its own velocity ( $v_t$ ), the relative position ( $\Delta p_t$ ) to immediate leader HV and relative velocity ( $\Delta v_t$ ) with respect to its immediate leader HV, and the predicted congestion stage ( $c_t$ ) from the congestion classifier ( $f_{\text{CC}}$ ):

$$o_t = [v_t, \Delta p_t, \Delta v_t] \oplus c_t, \\ c_t = f_{\text{CC}}(\{r_{p,i}, r_{v,i}\}_{i \in \mathcal{Z}}),$$

where  $\mathcal{Z}$  denotes the set of  $|\mathcal{Z}| = n$  vehicles within the sensing zone (55 m), and  $r_{p,i}$  and  $r_{v,i}$  are the relative position and velocity of the  $i$ -th vehicle, respectively.

- **Action.** The RV's action ( $a_t$ ) is its acceleration, bounded within  $[-3, 3]$  m/s<sup>2</sup>.
- **Reward.** The reward function  $R(s_t, a_t)$  is a weighted sum of the RV's velocity  $v_t$  (for the *efficiency* RV) or the

average velocity of all vehicles  $\bar{v}_t$  (for the *safety* RV), an acceleration penalty, and a shaping term based on the predicted congestion stage  $c_t$ .

---

#### Reward Functions

---

*efficiency* RV

$$R(s_t, a_t) = 0.75\bar{v}_t - 2|a_t|$$

**if**  $c_t = \text{Congested} \wedge a_t > 0$  **then**  
 $R(s_t, a_t) += \min(-1, \lambda_1|a_t|)$

**if**  $c_t = \text{Leaving} \wedge a_t < 0$  **then**  
 $R(s_t, a_t) += \lambda_2|a_t|$

*safety* RV

$$R(s_t, a_t) = 0.15\bar{v}_t - 4|a_t|$$

**if**  $c_t = \text{Forming}$  **then**  
 $R(s_t, a_t) += \min(-1, \lambda_3|a_t|)$

---

where  $\bar{v}_t = \frac{1}{n} \sum_{i=1}^n v_{i,t}$  is the average velocity of all  $n$  vehicles at time  $t$ , and  $\lambda_1 = -10$ ,  $\lambda_2 = -10$ , and  $\lambda_3 = -5$  are empirically determined weights.

- **Scaling laws.** Above 5% penetration, our RVs form platoons with a single leader and multiple followers. For instance, at 40% penetration, the platoon consists of 9 RVs ( $22 \times 0.4 = 8.8 \approx 9$ ), with a leader RV trained at 5% penetration and 8 followers. The follower RVs observe the platoon’s state (position and velocity of all vehicles in the platoon) and optimize the following reward:

$$R_{\text{follower}}(s_t, a_t) = \lambda_4 \Delta p_{t,j} + \lambda_5 \Delta v_{t,j} + \lambda_6 |a_{t,j}| + \lambda_7,$$

where  $\Delta p_{t,j}$  and  $\Delta v_{t,j}$  are the relative position and velocity of the  $j$ -th follower with respect to the leader,  $a_{t,j}$  is the follower’s acceleration, and  $\lambda_4 = -2$ ,  $\lambda_5 = 4$ ,  $\lambda_6 = -4$ , and  $\lambda_7 = 10$  are empirically chosen weights.

1) *Congestion Classifier:* Our RL-based approach employs a congestion classifier, a neural network trained with supervised learning to predict the congestion stage 10 time-steps in advance to allow for pre-emptive responses from our RV. The input features consist of the positions and velocities of preceding cars within the sensing zone which are mapped to one of six labels, each representing a distinct stage of congestion based on the asymmetric driving theory [42]. The theory suggests human drivers underestimate the required space headway during deceleration and overestimate it during acceleration. Consequently, when congestion is forming, the available space headway decreases monotonically from one vehicle to the next as we move downstream within the sensing zone. Conversely, when congestion is dissipating, the available space headway increases monotonically. The six labels used to capture the congestion stages are: ‘Forming’, ‘Leaving’, ‘Congested’, ‘Free flow’, ‘Undefined’, and ‘No Vehicle’, a subset of the labels are shown in Fig. 2.

To train the congestion classifier, we collect the position and velocity of all the vehicles inside the RV’s sensing zone (set to 55 m) at traffic density ranges [70 – 133] veh/km. The collected data is then clustered into six classes using the K-means algorithm, as shown in Fig.3 (RIGHT), where the dispersion of clusters indicates the classifiability of the data. Considering the sequential nature of the data and the requirement for making predictions multiple time-steps

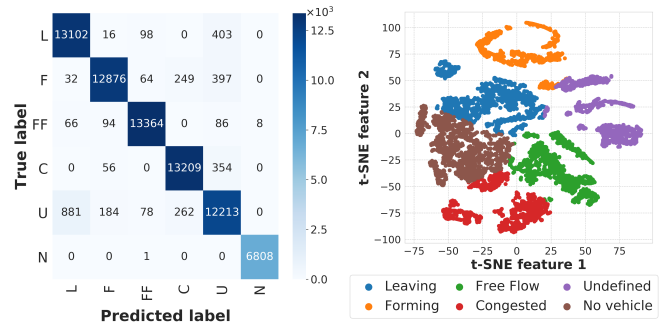


Fig. 3: LEFT: Confusion Matrix of a trained congestion classifier in Ring on the validation set with the six classes abbreviated as: L=‘Leaving’, F=‘Forming’, FF=‘Free Flow’, C=‘Congested’, U=‘Undefined’, and N=‘No Vehicle’. RIGHT: The results of applying K-means clustering with t-SNE on a subset of the training data of the congestion classifier. The clusters are spread out and distinct suggesting that the data is easily classifiable.

ahead, we choose a time offset of 10 time-steps. This offset strikes a balance between the usefulness and accuracy of the predictions. A larger offset, such as 100 time-steps, would provide more time for the RV to react, but the prediction is likely to be inaccurate, whereas a shorter offset, such as 1 time-step, would result in accurate predictions but may not allow sufficient time for the RV to take effective action.

After windowing, the dataset includes instances where the congestion stage changes from  $t$  to  $t + 10$ , as well as instances where the congestion stage remains the same over the time window. To train the congestion classifier, we sample data to ensure a balanced representation of transition/non-transition instances as well as instances containing all six classes. Worth noting, the ‘No vehicle’ class presents a unique challenge. The collected data may contain instances changing from ‘No vehicle’ to another class after the 10 time-steps. However, based on the input corresponding to ‘No vehicle’ at  $t$ , we cannot predict the congestion stage at  $t + 10$ . Consequently, we discard data points where the ‘No Vehicle’ class transitions to another class after 10 time-steps and replace them with synthetic examples that simulate various scenarios for the RV’s position and velocity without leader vehicles. The congestion classifier is trained for 50 epochs with validation accuracy of 95.5% (training parameters are provided in Table I and the confusion matrix on a validation set is shown in Fig. 3 LEFT). Finally, We incorporate the predictions of the congestion classifier into the observations and reward function of the RV.

2) *Benchmarking RL Policies:* To benchmark with other RL techniques, we reproduce them by following the provided experiment parameters and closely matching the performance. Specifically, to obtain RL policy with only local observations, we follow Wu et al. [43] and refer the policy as Wu hereafter; Our reproduced Wu achieves the performance within 1% error (measured with stabilization time and average velocity during stabilization) of the original work.

#### E. Perturbations Via Imitation Learning and Sampling

To ensure an accurate reproduction of real-world driving behaviors and perturbations in the simulation, we adopt a hy-

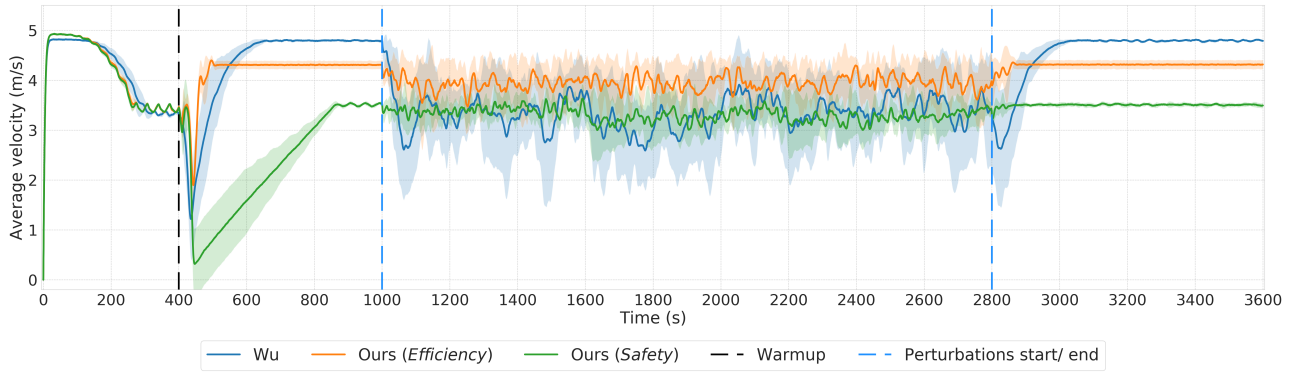


Fig. 4: Average velocity profile of RL-based approaches at 5% penetration under long-term application of real-world perturbations (for 30 minutes from 1000 s to 2800 s), averaged over 10 simulation rollouts. The solid lines indicate average velocity and colored ranges indicate standard deviation across rollouts. During the application of perturbations, Our *efficiency* RV has the highest average velocity at 3.95 m/s contributing to more throughput whereas Wu has the highest standard deviation at 1.35 m/s, indicating more sensitivity.

brid technique combining imitation learning and probabilistic sampling. We extract relevant real-world HV data during car-following such as ego velocity, headway distance, and leader velocity corresponding to the instantaneous accelerations shown in Fig. 1 TOP. We then train a behavioral cloning model represented by an 801-parameter neural network with these variables as input, acceleration command as predicted output, and real-world accelerations as expert demonstrations. The model minimizes the following objective:

$$\text{MSE} = \frac{1}{N} \sum_{i=1}^N (a_i - \hat{a}_i)^2$$

where  $N$  is the number of samples,  $a_i$  is the real-world acceleration, and  $\hat{a}_i$  is the predicted acceleration. To inject acceleration perturbations to HVs in simulation, we characterize the discrete acceleration behaviors extracted from the dataset in terms of intensity, frequency, and duration. Upon analysis, we find a negative correlation of intensity with frequency and durations i.e., higher intensity accelerations tend to have shorter duration and occur less frequently. Then, we uniformly sample the frequency of the perturbations within the observed range of [10, 30] per HV, for every 6 minutes of car-following. The intensity of the acceleration perturbations is determined based on the space headway of the HV. When the space headway is less than 5 m, human driving behavior becomes more sensitive, as the consequences of accelerations are more significant at shorter distances; hence, the accelerations are obtained from the imitation learning model to better capture the nuances of human driving. whereas if the we space headway is greater than 5 m, we sample acceleration intensity uniformly within  $[-3, 3] m/s^2$ . To determine the duration ( $\tau_{a_i}$ ) of each selected intensity  $a_i$ , we first find the most common duration (mode)  $\tilde{\tau}_{a_i}$  by linearly mapping  $a_i$  within the minimum ( $\tau_{\min}$ ) and maximum ( $\tau_{\max}$ ) observed durations. We then sample  $\tau_{a_i}$  from a piecewise triangular distribution using the following conditional probability density function:

$$P(\tau_{a_i} | \tilde{\tau}_{a_i}) = \begin{cases} \frac{2(\tau_{a_i} - \tau_{\min})}{\tau_{\text{range}}(\tilde{\tau}_{a_i} - \tau_{\min})}, & \tau_{\min} \leq \tau_{a_i} < \tilde{\tau}_{a_i}, \\ \frac{2(\tau_{\max} - \tau_{a_i})}{\tau_{\text{range}}(\tau_{\max} - \tilde{\tau}_{a_i})}, & \tilde{\tau}_{a_i} \leq \tau_{a_i} \leq \tau_{\max}. \end{cases}$$

where  $\tau_{\text{range}} = \tau_{\max} - \tau_{\min}$ . The sampled acceleration perturbation is randomly assigned to HVs during experiments.

Category	Parameter	Value
Simulation	Time Step ( $\Delta t$ )	0.1
	Simulation Horizon ( $T$ )	4500
	Warmup Time-steps	2500
	Speed Limit ( $m/s$ )	30
	Initial Speed ( $m/s$ )	0
PPO Algorithm	Learning Rate ( $\alpha$ )	0.00005
	Discount Factor ( $\gamma$ )	0.999
	GAE Estimation ( $\lambda$ )	0.97
	KL Divergence Target	0.02
	Entropy Coefficient Initial	0.1
Congestion Classifier	Entropy Coefficient Final	0.01
	Value Function Clip Param	20
	SGD Iterations	2
Policy Networks	Neural Network	32, 16, 16
	Batch Size	32
	Learning Rate	0.01
Policy Networks	Epochs	50
	Our Leader RV	64, 32, 16
Policy Networks	Our Follower RV	64, 32, 16
	Wu	32, 32, 32

TABLE I: Detailed experiment parameters. We show the simulation parameters as well as the parameters of Proximal Policy Optimization (PPO) and the congestion classifier. The hidden layer dimensions of various policy networks are also shown.

### III. EXPERIMENTS

We introduce the mixed traffic environment, the evaluation metrics, the experimental setup, and finally the results. To begin with, we test on the mixed traffic environment, the Ring: a single-lane circular road network with 22 vehicles as shown in Table II. This classical scene simulates ‘stop-and-go traffic’ where repeated cycles of accelerations and decelerations occur in HVs even in the absence of external disturbances. For our evaluations, we measure safety using surrogate measures associated with near-crash events, including Time to Collision (TTC  $\uparrow$ ) [44] to indicate collision risk and Deceleration Rate to Avoid a Crash (DRAC  $\downarrow$ ) [45] to quantify necessary braking force to avoid a collision. For

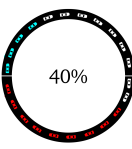
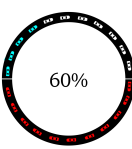
RV%	RV Type	Safety		Efficiency	
		TTC	DRAC	FE	Throughput
	IDM*	1.82 ± 0.23	1.62 ± 0.56	7.63 ± 0.23	988 ± 9.80
	FS	3.99 ± 0.77	0.89 ± 0.27	12.34 ± 0.54	1283 ± 42.44
	PlwS	1.95 ± 1.57	1.89 ± 0.88	12.99 ± 0.57	1343 ± 62.62
	BCM	1.03 ± 0.00	2.82 ± 0.10	8.17 ± 0.19	1023 ± 14.87
	LACC	1.09 ± 0.01	1.42 ± 0.03	8.01 ± 0.12	1031 ± 15.13
	Wu	2.39 ± 0.42	1.23 ± 0.39	9.92 ± 0.66	1048 ± 82.19
	<b>Ours</b>	<b>7.95 ± 2.29</b>	<b>0.36 ± 0.10</b>	<b>12.8 ± 0.72</b>	<b>1242 ± 51.34</b>
	FS	4.22 ± 0.55	0.74 ± 0.26	12.08 ± 0.61	1344 ± 29.39
	PlwS	1.71 ± 0.18	1.48 ± 0.42	11.76 ± 0.51	1328 ± 51.73
	BCM	2.21 ± 1.40	0.75 ± 0.30	13.19 ± 0.36	1392 ± 18.87
	LACC	1.08 ± 0.04	1.73 ± 0.09	9.42 ± 0.32	1166 ± 20.59
	Wu	2.24 ± 0.3	1.27 ± 0.24	6.41 ± 0.17	791 ± 62.52
	<b>Ours</b>	<b>5.84 ± 2.96</b>	<b>0.59 ± 0.28</b>	<b>12.87 ± 0.64</b>	<b>1336 ± 60.03</b>
	FS	3.53 ± 1.30	1.02 ± 0.60	11.55 ± 0.56	1323 ± 69.43
	PlwS	1.58 ± 0.16	1.89 ± 0.32	11.09 ± 0.54	1294 ± 65.91
	BCM	4.35 ± 6.61	0.7 ± 0.36	11.96 ± 0.42	1400 ± 10.95
	LACC	3.14 ± 2.34	0.90 ± 0.74	14.39 ± 0.40	1426 ± 30.07
	Wu	2.18 ± 0.43	1.27 ± 0.40	3.66 ± 0.16	456 ± 244.71
	<b>Ours</b>	<b>4.22 ± 2.08</b>	<b>0.89 ± 0.52</b>	<b>14.06 ± 0.45</b>	<b>1430 ± 75.63</b>
	FS	2.39 ± 0.64	1.00 ± 0.05	9.99 ± 0.55	1124 ± 170.60
	PlwS	1.59 ± 0.30	1.94 ± 0.53	10.70 ± 0.54	1264 ± 44.99
	BCM	2.29 ± 1.12	0.97 ± 0.67	11.79 ± 0.49	1393 ± 6.40
	LACC	2.55 ± 1.26	1.47 ± 1.42	13.91 ± 0.55	1448 ± 9.80
	Wu	2.83 ± 1.46	1.17 ± 0.42	4.41 ± 0.10	556 ± 240.38
	<b>Ours</b>	<b>6.58 ± 2.47</b>	<b>0.57 ± 0.27</b>	<b>13.61 ± 0.54</b>	<b>1473 ± 30.02</b>

TABLE II: Evaluation of RVs at various penetrations (RV/s are shown in red, observed human vehicles (HVs) are shown in cyan, and remaining HVs are white) averaged over 10 random rollouts with values after  $\pm$  indicating standard deviation. IDM\* denotes the 100% HV baseline. Ours highlighted in bold with results of the *efficiency* and *safety* RVs shown Safety and Efficiency columns respectively. Across all penetrations, our *safety* RV outperforms other methods in safety, exceeding the critical 4 s TTC threshold and reducing DRAC by up to 80% compared to IDM, with the exception of 40% penetration where it achieves the second-best performance in DRAC. Our *efficiency* RV improves the throughput by up to 49% (at 60% penetration) compared to IDM, while consistently maintaining the second-highest fuel economy among all evaluated RVs, with improvement of up to 84% at 40% penetration.

efficiency, Fuel Economy (FE  $\uparrow$ ) measures the miles driven per gallon of fuel consumed using the Handbook Emission Factors for Road Transport 3 Euro 4 passenger car emission model [46], while Throughput ( $\uparrow$ ) indicates network capacity utilization (flow rate).

For experiment setup, we use FLOW [43] and SUMO [19] with RVs platooned when penetration rate is  $> 5\%$  (all evaluated RVs can stabilize traffic in a platoon configuration, BCM and LACC require minimum 20% and 40% penetration respectively [27]). We select penetration rates 5%, 20%, 40%, and 60% to align with the minimum rates required for stabilizing traffic by different RVs [27], [47]. We adhere to stringent safety standards in our evaluations of TTC, DRAC hence when multiple RVs are present, we report the worst-case values among the RVs (including IDM baseline where the worst case among all vehicles is considered). In contrast, to measure efficiency we consider all vehicles in the network. In each experiment, we first allow the RV enough time to stabilize traffic and then we introduce acceleration perturbations for six-minute equivalent of real-world time.

Fig. 4 shows the velocity profiles of RL-based approaches in our study, namely Wu, Our *efficiency* RV, and Our *safety* RV at 5% penetration. All vehicles in the network are controlled using IDM during the initial 400 s of warmup time before the activation of RVs. After activation, Wu stabilizes traffic at 640 s, Our *efficiency* RV stabilizes traffic faster

than Wu at 595 s whereas Our *safety* RV stabilizes traffic gradually at 890 s. During stabilization, Wu maintains a higher average velocity of 4.88 m/s compared to Our *efficiency* RV at 4.37 m/s, while our *safety* RV has the lowest average velocity at 3.48 m/s. However, when perturbations are applied to HVs between 1000 s and 2800 s, Our *efficiency* RV maintains a higher average velocity at 3.95 m/s compared to Wu at 3.35 m/s while Our *safety* RV at 3.31 m/s has comparable average velocity to Wu. Notably, between 1000 s and 2800 s, Wu has the highest standard deviation of 1.35 m/s compared to Our *efficiency* RV at 0.80 m/s and Our *safety* RV at 0.70 m/s, indicating more sensitivity to applied perturbations.

Table II presents comparative evaluation of various RVs in the Ring at 85 veh/km density. Across all penetration rates, our *safety* RV consistently outperforms other methods in terms of TTC. Importantly, only our RV manages to exceed the critical 4 s threshold for TTC at all penetration rates, a threshold that is often used to activate automatic collision avoidance systems or warn drivers [48] and has also been recommended by earlier studies [44], [49]. Additionally, DRAC is reduced by up to 80% (at 5% penetration) in comparison to IDM and Our *safety* RV delivers the lowest DRAC at all penetrations except at 40%. Similarly, Our *efficiency* RV achieves the highest throughput at higher penetration rates

(improvements of 44% and 49% at penetration rates 40% and 60% respectively, compared to IDM). Furthermore, Our *efficiency* RV improves fuel economy up to 84% (at 60% penetration) and is consistently the second highest among all other RVs at all penetration rates.

#### IV. CONCLUSION AND FUTURE WORK

In this work, we combine imitation learning and probabilistic sampling to address the *Sim2Real* gap in modeling human driving behavior for mixed traffic control. Further, we propose a novel approach for optimizing safety and efficiency in mixed traffic using reinforcement learning-based robot vehicles (RVs) by introducing CARL with two classes of RVs: *safety* RV and *efficiency* RV, both leveraging a classifier to predict congestion stage in advance. Through extensive experiments in the Ring with injected real-world perturbations, we demonstrate that our RV is able to increase the time to collision (TTC) above the critical 4 s threshold, reduce the deceleration rate to avoid a crash (DRAC) by up to 80%, and increase throughput up to 49%. CARL is practical for real-world deployment as it relies on sensors like LiDAR which have a fixed maximum sensing range. However, additional experiments involving real hardware are needed to fully validate its scalability and robustness.

There are also potential ethical implications regarding the safety and privacy of human drivers interacting with RVs deployed in mixed traffic that merit further investigation. CARL inherently addresses the privacy issues as our approach prioritizes privacy by design. During the interaction between human drivers and RVs, our sensing relies on position and velocity, and does not collect sensitive information related to human drivers that could be traced back to their identity. However, a dedicated effort to investigate privacy concerns is crucial to ensure that data collected by RVs is anonymized and used responsibly.

In future work, we plan to incorporate additional traffic dynamics such as lane-changing and heterogeneous vehicle types. We also aim to conduct generalization studies in more complex environments like intersections [50]. Additionally, we plan to perform control and coordination at a city-wide scale by relying on network-wide traffic state prediction and evaluate the robustness of such approaches [51]. Similarly, applying our approach on real hardware, including micro-mobility vehicles [52], is also an interesting future direction.

#### ACKNOWLEDGEMENT

This research is supported by NSF 2153426, 2129003, and 2038967. The authors would also like to thank NVIDIA and the Center for Transportation Research (CTR) at the University of Tennessee, Knoxville for their support.

#### REFERENCES

- [1] USDOT's automated vehicles comprehensive plan, 2024.
- [2] U.S. Environmental Protection Agency' green vehicle guide on self-driving vehicles, 2024.
- [3] Raunak P Bhattacharyya, Derek J Phillips, Blake Wulfe, Jeremy Morton, Alex Kuefler, and Mykel J Kochenderfer. Multi-agent imitation learning for driving simulation. in 2018 ieee. In *RSJ International Conference on Intelligent Robots and Systems (IROS)*, pages 1534–1539.
- [4] Alex Kuefler, Jeremy Morton, Tim Wheeler, and Mykel Kochenderfer. Imitating driver behavior with generative adversarial networks. In *2017 IEEE intelligent vehicles symposium (IV)*, pages 204–211. IEEE, 2017.
- [5] Xuan Di and Rongye Shi. A survey on autonomous vehicle control in the era of mixed-autonomy: From physics-based to ai-guided driving policy learning. *Transportation research part C: emerging technologies*, 125:103008, 2021.
- [6] Michael Villarreal, Bibek Poudel, Jia Pan, and Weizi Li. Mixed traffic control and coordination from pixels. In *IEEE International Conference on Robotics and Automation (ICRA)*, 2024.
- [7] Michael Villarreal, Dawei Wang, Jia Pan, and Weizi Li. Analyzing emissions and energy efficiency in mixed traffic control at unsignalized intersections. In *IEEE Forum for Innovative Sustainable Transportation Systems (FISTS)*, 2024.
- [8] Michael Villarreal, Bibek Poudel, and Weizi Li. Can chatgpt enable its? the case of mixed traffic control via reinforcement learning. In *IEEE International Conference on Intelligent Transportation Systems (ITSC)*, pages 3749–3755, 2023.
- [9] Dawei Wang, Weizi Li, Lei Zhu, and Jia Pan. Learning to control and coordinate mixed traffic through robot vehicles at complex and unsignalized intersections. *arXiv preprint arXiv:2301.05294*, 2023.
- [10] Dawei Wang, Weizi Li, and Jia Pan. Large-scale mixed traffic control using dynamic vehicle routing and privacy-preserving crowdsourcing. *IEEE Internet of Things Journal*, 11(2):1981–1989, 2024.
- [11] Bibek Poudel, Weizi Li, and Kevin Heaslip. Endurl: Enhancing safety, stability, and efficiency of mixed traffic under real-world perturbations via reinforcement learning. *arXiv preprint*, 2024.
- [12] Jeffrey Hawke, Richard Shen, Corina Gurau, Siddharth Sharma, Daniele Reda, Nikolay Nikolov, Przemysław Mazur, Sean Micklethwaite, Nicolas Griffiths, Amar Shah, et al. Urban driving with conditional imitation learning. In *2020 IEEE International Conference on Robotics and Automation (ICRA)*, pages 251–257. IEEE, 2020.
- [13] Duo Zhang, Xiaoyun Chen, Junhua Wang, Yinhai Wang, and Jian Sun. A comprehensive comparison study of four classical car-following models based on the large-scale naturalistic driving experiment. *Simulation Modelling Practice and Theory*, 113:102383, 2021.
- [14] Nathan Lichtlé, Eugene Vinitsky, Matthew Nice, Benjamin Seibold, Dan Work, and Alexandre M Bayen. Deploying traffic smoothing cruise controllers learned from trajectory data. In *2022 International Conference on Robotics and Automation (ICRA)*, pages 2884–2890. IEEE, 2022.
- [15] Peter G Gipps. A behavioural car-following model for computer simulation. *Transportation research part B: methodological*, 15(2):105–111, 1981.
- [16] Stefan Krauß. Microscopic modeling of traffic flow: Investigation of collision free vehicle dynamics. 1998.
- [17] Martin Treiber and Arne Kesting. Traffic flow dynamics. *Traffic Flow Dynamics: Data, Models and Simulation*, Springer-Verlag Berlin Heidelberg, pages 983–1000, 2013.
- [18] Saleh Albeaik, Alexandre Bayen, Maria Teresa Chiri, Xiaoqian Gong, Amaury Hayat, Nicolas Kardous, Alexander Keimer, Sean T McQuade, Benedetto Piccoli, and Yiling You. Limitations and improvements of the intelligent driver model (idm). *SIAM Journal on Applied Dynamical Systems*, 21(3):1862–1892, 2022.
- [19] Pablo Alvarez Lopez, Michael Behrisch, Laura Bieker-Walz, Jakob Erdmann, Yun-Pang Flötteröd, Robert Hilbrich, Leonhard Lücken, Johannes Rummel, Peter Wagner, and Evamarie Wießner. Microscopic traffic simulation using sumo. In *2018 21st international conference on intelligent transportation systems (ITSC)*, pages 2575–2582. IEEE, 2018.
- [20] Martin Treiber and Arne Kesting. The intelligent driver model with stochasticity-new insights into traffic flow oscillations. *Transportation research procedia*, 23:174–187, 2017.
- [21] Arne Kesting and Martin Treiber. Calibrating car-following models by using trajectory data: Methodological study. *Transportation Research Record*, 2088(1):148–156, 2008.
- [22] Li Li, Xiquan Micheal Chen, and Lei Zhang. A global optimization algorithm for trajectory data based car-following model calibration. *Transportation Research Part C: Emerging Technologies*, 68:311–332, 2016.
- [23] MN Sharath and Nagendra R Velaga. Enhanced intelligent driver model for two-dimensional motion planning in mixed traffic. *Transportation Research Part C: Emerging Technologies*, 120:102780, 2020.
- [24] Meixin Zhu, Xuesong Wang, Andrew Tarko, et al. Modeling car-following behavior on urban expressways in shanghai: A naturalistic

- driving study. *Transportation research part C: emerging technologies*, 93:425–445, 2018.
- [25] Cathy Wu, Aboudy Kreidieh, Kanaad Parvate, Eugene Vinitsky, and Alexandre M Bayen. Flow: Architecture and benchmarking for reinforcement learning in traffic control. *arXiv preprint arXiv:1710.05465*, 10, 2017.
- [26] Abdul Rahman Kreidieh, Cathy Wu, and Alexandre M Bayen. Dissipating stop-and-go waves in closed and open networks via deep reinforcement learning. In *2018 21st International Conference on Intelligent Transportation Systems (ITSC)*, pages 1475–1480. IEEE, 2018.
- [27] Fang-Chieh Chou, Alben Rome Bagabaldo, and Alexandre M Bayen. The lord of the ring road: a review and evaluation of autonomous control policies for traffic in a ring road. *ACM Transactions on Cyber-Physical Systems (TCPS)*, 6(1):1–25, 2022.
- [28] Eugene Vinitsky, Aboudy Kreidieh, Luc Le Flem, Nishant Kheterpal, Kathy Jang, Cathy Wu, Fangyu Wu, Richard Liaw, Eric Liang, and Alexandre M Bayen. Benchmarks for reinforcement learning in mixed-autonomy traffic. In *Conference on robot learning*, pages 399–409. PMLR, 2018.
- [29] Mayuri Sridhar and Cathy Wu. Piecewise constant policies for human-compatible congestion mitigation. In *2021 IEEE International Intelligent Transportation Systems Conference (ITSC)*, pages 2499–2505. IEEE, 2021.
- [30] Xiao Wang, Rui Jiang, Li Li, Yilun Lin, Xinhua Zheng, and Fei-Yue Wang. Capturing car-following behaviors by deep learning. *IEEE Transactions on Intelligent Transportation Systems*, 19(3):910–920, 2017.
- [31] Meixin Zhu, Yinhai Wang, Ziyuan Pu, Jingyun Hu, Xuesong Wang, and Ruimin Ke. Safe, efficient, and comfortable velocity control based on reinforcement learning for autonomous driving. *Transportation Research Part C: Emerging Technologies*, 117:102662, 2020.
- [32] Meixin Zhu, Xuesong Wang, and Yinhai Wang. Human-like autonomous car-following model with deep reinforcement learning. *Transportation research part C: emerging technologies*, 97:348–368, 2018.
- [33] Tianyu Shi, Yifei Ai, Omar ElSamadisy, and Baher Abdulhai. Bilateral deep reinforcement learning approach for better-than-human car following model. *arXiv preprint arXiv:2203.04749*, 2022.
- [34] Raunak Bhattacharyya, Blake Wulfe, Derek J Phillips, Alex Kuefler, Jeremy Morton, Ransalu Senanayake, and Mykel J Kochenderfer. Modeling human driving behavior through generative adversarial imitation learning. *IEEE Transactions on Intelligent Transportation Systems*, 24(3):2874–2887, 2022.
- [35] Tianya Zhang, Peter J Jin, Sean T McQuade, and Benedetto Piccoli. Car-following models: A multidisciplinary review. *arXiv preprint arXiv:2304.07143*, 2023.
- [36] Luc Le Mero, Dewei Yi, Mehrdad Dianati, and Alexandros Mouzakis. A survey on imitation learning techniques for end-to-end autonomous vehicles. *IEEE Transactions on Intelligent Transportation Systems*, 23(9):14128–14147, 2022.
- [37] Derek Gloude-mans, Yanbing Wang, Junyi Ji, Gergely Zachar, William Barbour, Eric Hall, Meredith Cebelak, Lee Smith, and Daniel B Work. I-24 motion: An instrument for freeway traffic science. *Transportation Research Part C: Emerging Technologies*, 155:104311, 2023.
- [38] Raphael E Stern, Shumo Cui, Maria Laura Delle Monache, Rahul Bhadani, Matt Bunting, Miles Churchill, Nathaniel Hamilton, Hannah Pohlmann, Fangyu Wu, Benedetto Piccoli, et al. Dissipation of stop-and-go waves via control of autonomous vehicles: Field experiments. *Transportation Research Part C: Emerging Technologies*, 89:205–221, 2018.
- [39] Berthold KP Horn. Suppressing traffic flow instabilities. In *16th International IEEE Conference on Intelligent Transportation Systems (ITSC 2013)*, pages 13–20. IEEE, 2013.
- [40] Rajesh Rajamani. *Vehicle dynamics and control*. Springer Science & Business Media, 2011.
- [41] John Schulman, Filip Wolski, Prafulla Dhariwal, Alec Radford, and Oleg Klimov. Proximal policy optimization algorithms. *arXiv preprint arXiv:1707.06347*, 2017.
- [42] Hwasoo Yeo. *Asymmetric microscopic driving behavior theory*. University of California, Berkeley, 2008.
- [43] Cathy Wu, Abdul Rahman Kreidieh, Kanaad Parvate, Eugene Vinitsky, and Alexandre M Bayen. Flow: A modular learning framework for mixed autonomy traffic. *IEEE Transactions on Robotics*, 38(2):1270–1286, 2021.
- [44] Katja Vogel. A comparison of headway and time to collision as safety indicators. *Accident analysis & prevention*, 35(3):427–433, 2003.
- [45] Dale F Cooper and N Ferguson. Traffic studies at t-junctions. 2. a conflict simulation record. *Traffic Engineering & Control*, 17(Analytic), 1976.
- [46] Peter De Haan and Mario Keller. Modelling fuel consumption and pollutant emissions based on real-world driving patterns: the hbefta approach. *International journal of environment and pollution*, 22(3):240–258, 2004.
- [47] Bibek Poudel, Kevin Heaslip, and Weizi Li. Endurl: Enhancing safety, stability, and efficiency of mixed traffic under real-world perturbations via reinforcement learning. *arXiv preprint arXiv:2311.12261*, 2023.
- [48] Michiel M Minderhoud and Piet HL Bovy. Extended time-to-collision measures for road traffic safety assessment. *Accident Analysis & Prevention*, 33(1):89–97, 2001.
- [49] TJ Ayres, L Li, David Schleuning, and D Young. Preferred time-headway of highway drivers. In *ITSC 2001. 2001 IEEE Intelligent Transportation Systems. Proceedings (Cat. No. 01TH8585)*, pages 826–829. IEEE, 2001.
- [50] Dawei Wang, Weizi Li, Lei Zhu, and Jia Pan. Learning to control and coordinate mixed traffic through robot vehicles at complex and unsignalized intersections. *arXiv preprint arXiv:2301.05294*, 2023.
- [51] Bibek Poudel and Weizi Li. Black-box adversarial attacks on network-wide multi-step traffic state prediction models. In *2021 IEEE International Intelligent Transportation Systems Conference (ITSC)*, pages 3652–3658. IEEE, 2021.
- [52] Bibek Poudel, Thomas Watson, and Weizi Li. Learning to control dc motor for micromobility in real time with reinforcement learning. In *2022 IEEE 25th International Conference on Intelligent Transportation Systems (ITSC)*, pages 1248–1254. IEEE, 2022.